Jurnal Tribologi 20 (2019) 51-64

Jurnal Tribologi
Website : jurnaltribologi.mytribos.org
e-issn: 2289-7232

An experimental compression test of lubricants with direct measurement of lubricant pressure build-up

Sulaiman, M.H. [1,*], Christiansen, P. [2], Bay, N. [2]

[1] Division of Design and Manufacturing, Universiti Malaysia Perlis, 02600 Arau, Perlis, MALAYSIA.
[2] Department of Mechanical Engineering, Technical University of Denmark, 2800 Kgs. Lyngby, DENMARK.
[*]Corresponding author: hafissulaiman@unimap.edu.my

KEYWORD

Direct measurement
Compressibility
Bulk modulus
High pressure
Lubricant

ABSTRACT

The influence of workpiece surface topography on friction, lubrication and final surface quality in metal forming operations is well known. This is especially the case when liquid lubricants are applied in situations where increased workpiece surface roughness facilitates the lubricant entrapment, pressurization and possible escape by Micro-Plasto-HydroDynamic Lubrication (MPHDL). In order to model this lubrication mechanism, an important lubricant property designated the *bulk modulus* is needed for characterizing the compressibility and the pressurization of the lubricant. This paper presents an experimental of direct measurement of the lubricant bulk modulus at pressure levels up to 500 MPa. The paper includes the design concept of the high-pressure equipment for the test as well as the experimental results. The bulk modulus of water as a test fluid was compared with literature values for validation of the equipment. Testing of different liquid lubricants for metal forming revealed a nonlinear relationship between the bulk modulus and the pressure.

Received 23 March 2018; received in revised form 20 July 2018; accepted 3 September 2018.
To cite this article: Sulaiman et al. (2019). An experimental compression test of lubricants with direct measurement of lubricant pressure build-up. Jurnal Tribologi 20, pp.51-64.

NOMENCLATURE

K	Bulk modulus of the lubricant
V	Volume of the lubricant, mm^3
p	Pressure of the lubricant, MPa
E	Elastic modulus, MPa
ν	Poisson ratio
ρ	Density, g/cm^3
η_v	Kinematic viscosity of the lubricant, cSt
τ	Friction stress, MPa
μ	Coulomb friction coefficient
HV	Hardness of the ring, kp/mm^2
σ_f	Flow stress of the ring, MPa
ε	Effective strain of the ring
σ_r	Radial stress of the die, MPa
A_o	Initial area of the inner die, mm^2
L_i	Punch stroke, mm
L	Punch stroke, mm
V/V_o	Relative volume of the lubricant
V_i	Volume of the lubricant, mm^3
V_o	Initial volume of the lubricant, mm^3
ΔV	Volume change of the lubricant, mm^3
Δr	Radial expansion of the die, mm
Δz	Vertical expansion of the punches, mm^3
F	Hydrostatic force of the lubricant, N
$MPHSL$	Micro-Plasto-HydroStatic Lubrication
$MPHDL$	Micro-Plasto-HydroDynamic Lubrication

1.0 INTRODUCTION

Metal forming in the mixed lubrication regime implies that the forming load in the tool/workpiece interface is shared between the metal-to-metal asperity contacts and the pressurized lubricant in the pockets between asperity contacts. Kudo, (1965) and Wanheim, (1973) pointed out that the large load carrying capacity of such enclosed pockets filled with lubricant resulting in poor surface quality with considerable reduction of friction. Theoretical models to determine the resulting contact area by considering the elastic compression of the liquid in the closed pockets were established by Kudo, (1965) and Nellemann et al., (1977). The concepts of Micro-Plasto-HydroStatic Lubrication (MPHSL) and Micro-Plasto-HydroDynamic Lubrication (MPHDL) were introduced by Mizuno and Okamoto (1982) and later verified by Kudo et al., (1982), Azushima et al. (1990), and Azushima and Kudo, (1995). Bech et al., (1998) have further investigated MPHDL and had set up a mathematical model to predict the onset of this

mechanism (Sorensen et al., 1999). Similar modelling was subsequently carried out by Lo and Wilson (1999), Azushima, (2000) and Stephany et al., (2005).

It is known that the lubricant volume V changes with the hydrostatic pressure, p (Nellemann et al., 1977). This changes are expressed by the bulk modulus K of the compressed lubricant as stated in Equation 1.

$$K = -V\frac{dp_{lub}}{dV} \tag{1}$$

From Equation 1, the calculation of the increased pressure of lubricant trapped in closed pockets of the workpiece surface in metal forming requires knowledge on the lubricant bulk modulus. These data are difficult to find in the literature, and the standard test methods require advanced laboratory equipment (Jacobson, 1991), (Ohno, 2007), (ASTM, 2012), (Bair et al., 2016). Most of the advanced laboratory equipment are able to determine the lubricant pressure indirectly by measuring the punch load outside the pressure chamber. However, the friction generated in the sealing during the force measurement leads to an overestimation of the pressure in the lubricant, see Figure 1. A simple laboratory test combined with an inverse Finite Element (FE) analysis to determine the lubricant bulk modulus was developed by the authors Sulaiman et al., (2016), but the methodology was only applicable to the low pressure range.

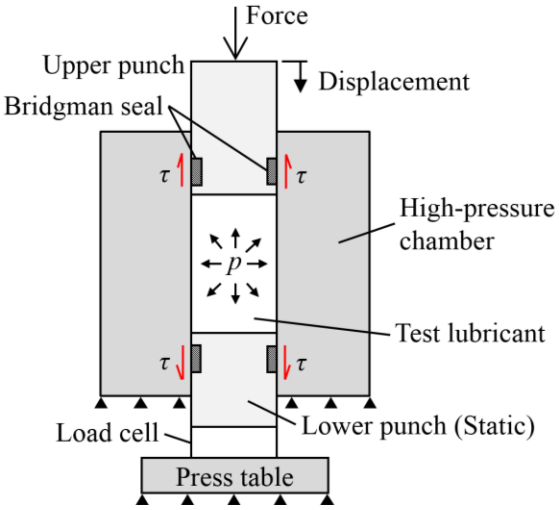

Figure 1: Illustration of the overestimated force due to the generated friction stress τ in the sealing from both upper and lower punches.

The present paper describes an experimental compression test of liquid lubricants with direct measurement of the lubricant pressure build-up and the subsequent determination of the lubricant bulk modulus in a wide pressure range. The work includes design and construction of a new, high-pressure compressibility equipment and testing of the liquid lubricant compressibility up to 500 MPa, i.e. in a pressure range similar to the one appearing in the tool-workpiece interface in stamping of stainless steel sheet (Ceron et al., 2014), (Sulaiman et al., 2018).

2.0 EXPERIMENTAL SETUP

A high-pressure compressibility equipment was designed and constructed to measure the lubricant pressure build-up with decreasing lubricant volume in a pre-stressed Ø37 mm high pressure container with two fitting punches, see Figure 2. During the test, the lower punch was stationary, whereas the upper punch was moving in order to compress the liquid between the punches. Load was delivered by a 2 MN hydraulic cylinder. Custom made Bridgman seals of the liquid were mounted on the punches. Figure 3 shows the seal components comprising of three rings; ring 1, ring 2 and ring 3. For testing of lubricants to 500 MPa, ring 1, which has a triangular cross section is made of copper, ring 2 with a square cross section is made of Teflon, whereas ring 3 is a commercial U-shaped rubber seal, Variseal M2S from Trelleborg, Sweden. A central bore in the bottom punch leads the oil to a pressure sensor (HBM, P3MBP BlueLine) and the measuring range is up to 1.5 GPa. The volume change was measured by a length transducer by measuring the punch travel (HBM, WA/50mm) and the measuring length range is up to 50 mm.

3.0 NUMERICAL ANALYSIS-OF HIGH-PRESSURE COMPRESSIBILITY EQUIPMENT

3.1 Tool deflection

A numerical analysis in LS-DYNA v. R7.1.1 was performed using implicit time integration to estimate the deflection of the tools under load by coupling deformation of the lubricant and metal, Figure 4(a). The axisymmetric finite element model was used with 9477 fully integrated, linear quadrilateral elements and the absolute tolerance is set to 1×10^{-3} in the simulation. The numerical solution is assumed converged when the iterations is smaller than a maximum value of 1×10^{-3}. A fine, uniform mesh was applied in the contact between the container, punches and the lubricant. The upper and lower punches as well as the pre-stressed container were modelled as elastic bodies in order to calculate the tool deflections and to compare the pressure build-up with punch stroke in both elastic and rigid models. The material properties are listed in Table 1. The test lubricant was treated as a fluid with a constant bulk modulus K = 2200 MPa. Coulomb friction $\tau = \mu p$ with μ=0.1 was assumed in all surface contacts.

Table 1: Tool materials and their properties.

Components	Material types	Properties		
		Density ρ (g/cm^3)	**Poisson Ratio ν**	**Elastic Modulus E (GPa)**
Punches	Uddeholm Unimax	7.8	0.3	213
Punch cap	Uddeholm Unimax	7.8	0.3	213
Die container	Uddeholm Vanadis 4E	7.7	0.3	206

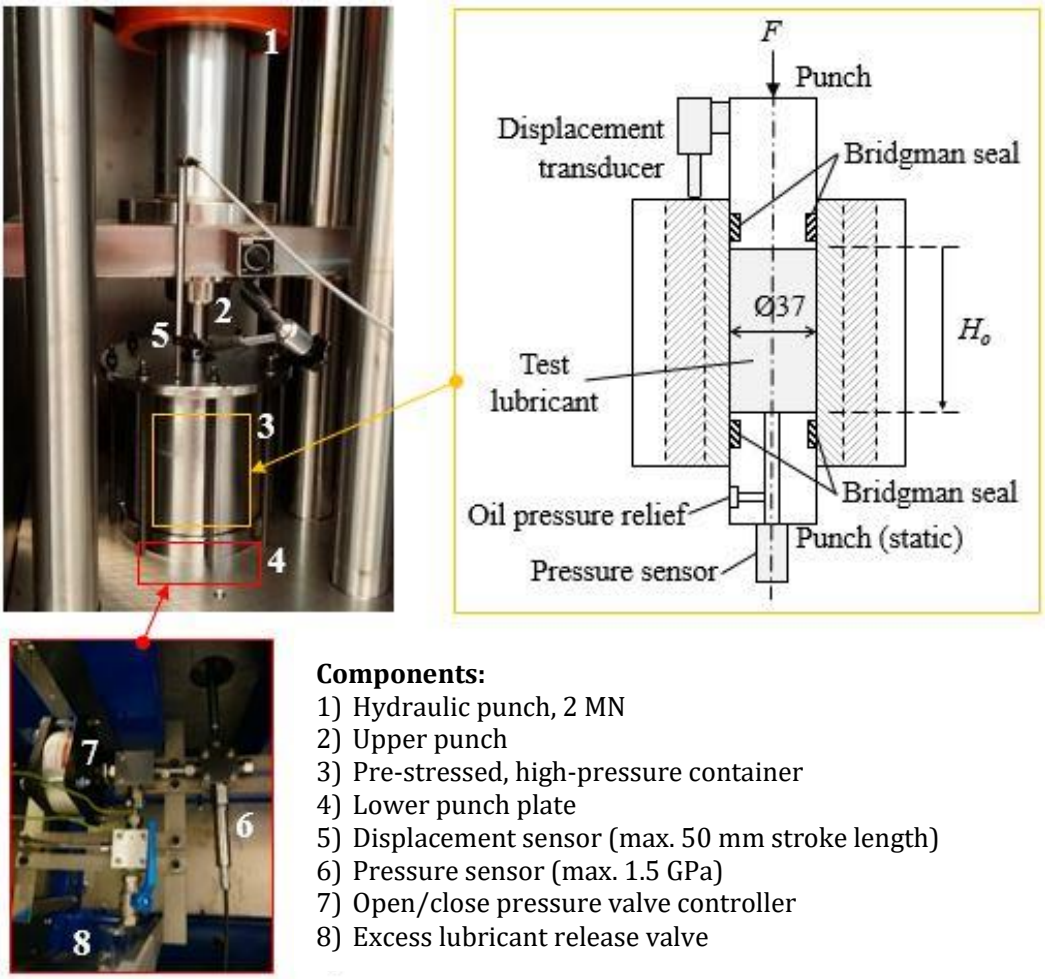

Components:
1) Hydraulic punch, 2 MN
2) Upper punch
3) Pre-stressed, high-pressure container
4) Lower punch plate
5) Displacement sensor (max. 50 mm stroke length)
6) Pressure sensor (max. 1.5 GPa)
7) Open/close pressure valve controller
8) Excess lubricant release valve

Figure 2: Schematics of components for measuring compressibility of liquid lubricants.

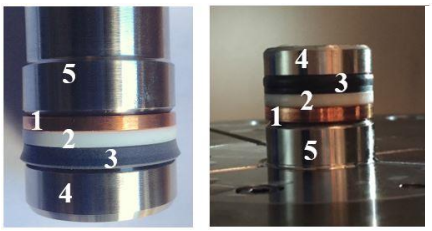

Components:
1) Ring 1 – Copper
2) Ring 2 – Teflon
3) Ring 3 – Commercial U-shaped seal
4) Punch cap
5) Punch

Figure 3: Bridgman seal on (a) upper and (b) lower punches.

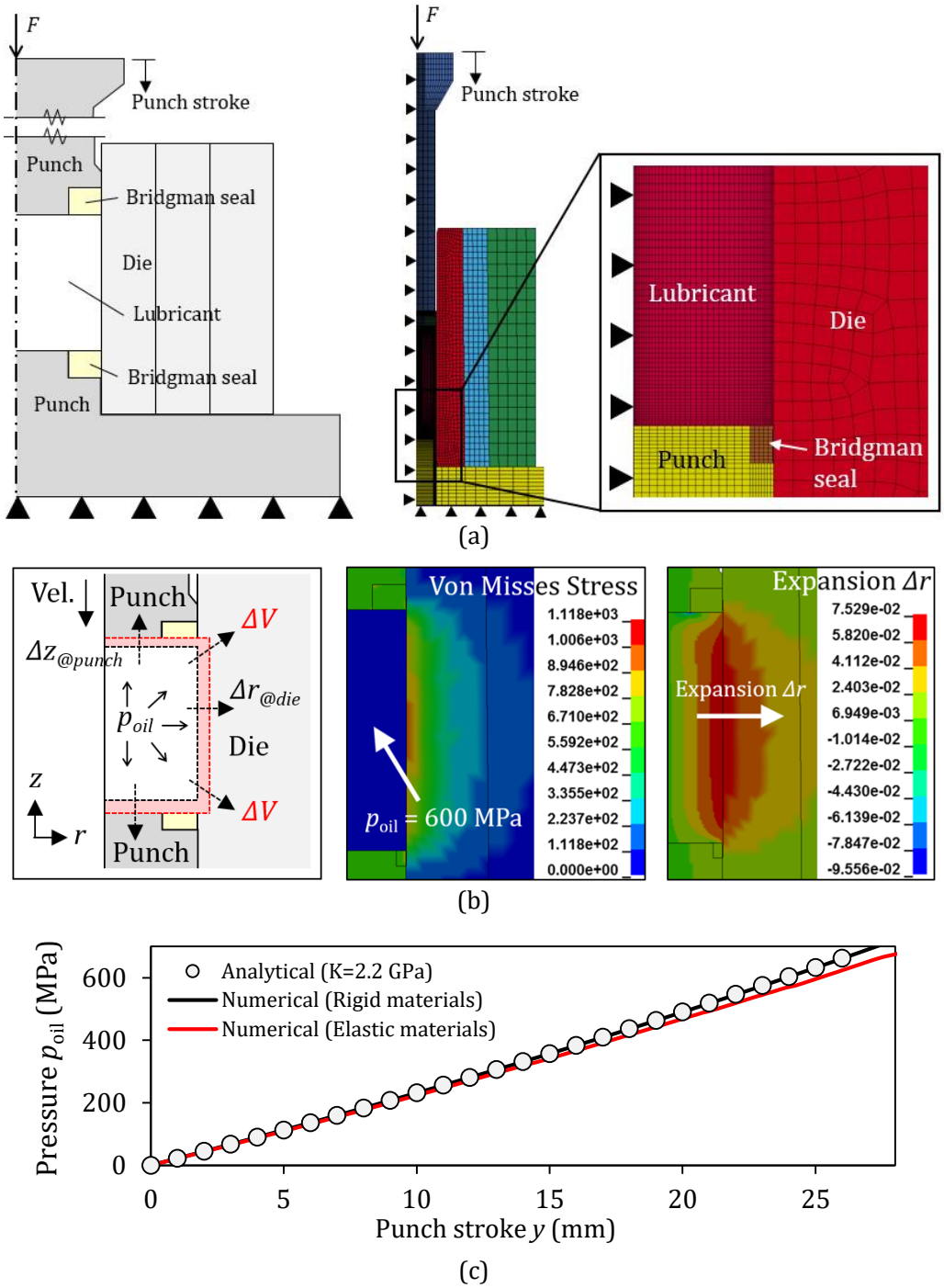

Figure 4: (a) Schematic of the numerical model simulating the lubricant compressibility test, (b) Expansion of the die (r-axis) and compression of punches (z-axis) due to the pressurized lubricant, and (c) comparison of pressure build-up with punch stroke assuming rigid and elastic tools.

The tool deflection is schematically displayed in Figure 4(b). The elastic deflection, which reduces the volume decreased of the trapped liquid, occurs in the radial direction of the die and in the axial direction of the punches. A comparison of the determined pressure versus punch stroke for elastic and rigid tools can be seen in Figure 4(c). It can be noticed that same punch stroke gave rise to almost the same pressure. Therefore, the error in determining bulk modulus disregarding elastic deflection of the tools will thus be insignificant in the pressure range 0 – 550 MPa, wherefore the elastic deflection of the tools is neglected in the following.

3.2 Leakage control in Bridgman seal

A schematic of the Bridgman seal in Figure 4(a) and Figure 4(b) shows the deformation of the copper ring under load. The seal was not allowed to extrude into the cylindrical part of the gap between the punch and the container. FE simulation of the seal deformation was performed by adopting an axisymmetric model with fully integrated, linear quadrilateral elements. In the simulation, ring 2 and ring 3 were assumed as rigid materials. Based on the measured hardness of the copper ring (ring 1) HV = 95 kp/mm^2, it was assumed as an elastic-plastic material with a linear stress-strain curve with flow stress $\sigma_f(\varepsilon) = \sigma_f(0) = 310$ MPa at an effective strain of $\varepsilon = 0$, while $\sigma_f(0.15) = 470$ MPa at $\varepsilon = 0.15$ according to ref. (Sundström, 1998).

In order to ensure sufficient sealing pressure to prevent lubricant leakage, the conical part of the punches and ring 1 were designed with an angle of 46° and 45° towards vertical, respectively. A further modification to the Bridgman seal was to blunt the triangle tip of ring 1 to avoid extrusion of copper into the clearance between the punch and die container at high pressures, see Figure 5(a) (left). The numerical analysis proved this to be an efficient solution with a fluid pressure up to 550 MPa, see Figure 5(a) (right). The observation of the copper ring shape obtained before and after the experiments at the same pressure confirmed this, as seen in Figure 5(b)–(c). On the other hand, excessive pressure applied may cause the extrusion of copper as seen in Figure 6. To prevent the punch getting stuck in the container during extraction, an anti-friction coating of MoS_2 was sprayed on the copper ring prior to each test.

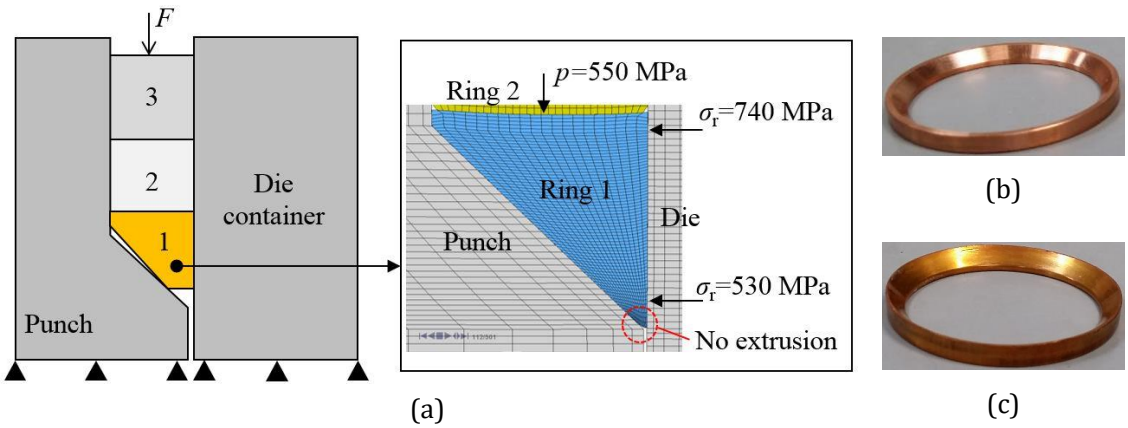

Figure 5: (a) Numerical analysis of ring seal compression describing a deforming copper ring at high pressure. The conical angle difference between copper ring and punch is enlarged for clarity. (b) Copper ring before the test, and (c) Copper ring after successful test, no extrusion at 550 MPa.

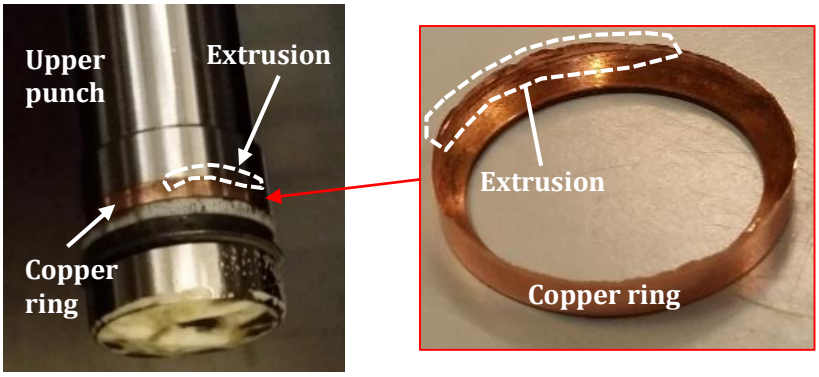

Figure 6: Extrusion of copper at excessive pressure.

4.0 EXPERIMENTAL PROCEDURE

First, the punch and inner die wall was cleaned from any remnants of lubricant, grease and other contaminants. 100 mL fluid was poured into a beaker and its volume was measured by a weight scale before it was transferred carefully into a container. The small remnants of fluid left in the beaker were measured by subsequent weighing. The actual weight and volume of fluid was then determined, see Table 2. The compressibility test was started by moving the upper punch slowly downwards thereby pressurizing the lubricant. During testing, the pressure and punch travel were recorded and saved in a LabView program. The test was stopped when the applied pressure reaches 500 MPa. The upper punch was slowly unloaded and the Bridgman seals on the punches were carefully checked for any possible damage. The seals were replaced if any damages occurred.

Table 2: Measured weight and calculated volume of the test fluids.

Lubricant types	Product name	Notation	Weight (g)	Volume (m*L*)
Water	-	Water	95.6	93.6
Pure mineral oil	CR5	CR5	83.0	90.2
Pure mineral oil	CR5-Sun 60*	CR5-Sun*	82.4	88.7
Mineral oil with additive	Rhenus LA722086	R800	96.4	87.1
Mineral oil with additive	Rhenus LA722083	R300	93.8	87.4
Chlorinated paraffin oil	TDN81	TDN81	107.6	99.3

** 50 wt. % mixture lubricant – Houghton Plunger CR5 (η=660 cSt) and Sunoco Sun 60 (η=10 cSt).*

5.0 TEST LUBRICANTS

Five different mineral oils were selected for the experiments, see Table 3. Most of the oils are common lubricants used in sheet stamping operations of high strength steel and stainless steel. Two of them – with medium and high viscosity, R300 and R800 respectively – contains additives with boundary lubrication properties. The other two are the mineral oils with no additives. One of them is a high viscous lubricant CR5, and the other one is a mixture of both mineral oils with no additives with a low viscous lubricant CR5-Sun*, giving a rather low, resulting viscosity. The last mineral oil used in this experiment is a chlorinated mineral oil TDN81, which is known to

efficiently prevent galling but also considered to be hazardous to personnel and environment. Data on the test lubricants are listed in Table 4.

Table 3: Test lubricant properties.

Properties	Product	Properties	
		Density ρ (g/cm³)	**Kinematic Viscosity η_v at 40°C (cSt)**
Pure mineral oil	CR5	0.92	660
Pure mineral oil	CR5-Sun*	0.93	60
Mineral oil with additive	R800	1.11	800
Mineral oil with additive	R300	1.07	300
Chlorinated paraffin oil	TDN81	1.20	150

** 50 wt. % mixture lubricant – Houghton Plunger CR5 (η=660 cSt) and Sunoco Sun 60 (η=10 cSt).*

In order to ensure that the high-pressure equipment is capable of measuring the compressibility of fluids accurately at high pressures, a verification was performed with water as a reference fluid. Properties of water at room temperature are listed in Table 4, where the bulk modulus of the water at ambient pressure is 2.2 GPa.

Table 4: Properties of water at room temperature.

Properties	**Value**	**Unit**
Density ρ	1.02	g/cm³
Kinematic viscosity η_v at 40 °C	0.658	cSt
Bulk modulus K at ambient pressure	2200	MPa

6.0 RESULTS AND DISCUSSION

6.1 Data treatment and verification of the test

The direct measurement of the liquid lubricant pressure builds up inside the high-pressure container allows for the direct determination of the bulk modulus at various pressure levels with no influence from friction generated between punch and container in the sealing. Figure 7(a) shows an example of the measured punch stroke – pressure curve for water. Matlab software was used to process the recorded data of pressure p vs. punch stroke L. A mathematical curve fit in form of a second order polynomium of pressure versus punch stroke was determined for each test in this method.

Using Equation 1 the bulk modulus K is determined as a function of the pressure. The liquid volume in stage i is given by:

$$V_i = A_o L_i \tag{2}$$

which implies:

$$dV_i = A_0 dL_i \tag{3}$$

Inserting in Equation 1 gives:

$$K_i = -L_i \frac{dp_i}{dL_i} \tag{4}$$

which implies that the bulk modulus can be determined as a function of the pressure by simple differentiation of the mathematical expression of the pressure-punch travel. By using the curve fit in Figure 7(a), the bulk modulus determined for water is shown in Figure 7(b). Figure 7(a) shows that the bulk modulus of water has increased non-linearly with pressure. A reasonable agreement was achieved with Hayward, (1967) for the bulk modulus of water at elevated pressures, especially at pressures above 100 MPa.

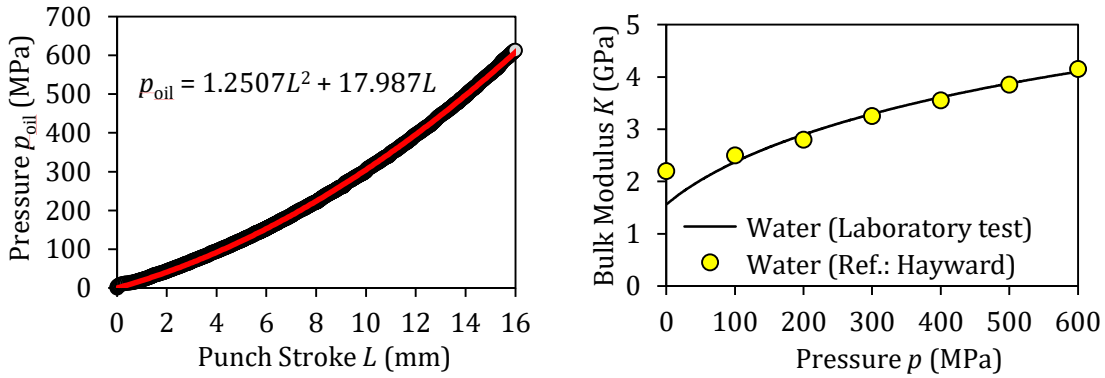

Figure 7: (a) Punch stroke – pressure curve for water, and (b) Compressibility of water at various pressure levels.

6.2 Pressure sensitivity of the lubricant bulk modulus *K*

Calculation of the pressure sensitivity of the lubricant bulk modulus are evaluated from the direct measurement of the lubricant pressure build up and punch stroke measurement. This includes subsequent computation utilizing a mathematical curve fit in the form of a second order polynomium of pressure versus punch stroke as described above. Figure 8(a) shows the measured volume change at various pressure levels. It can be seen that the chlorinated paraffin oil TDN81 have less compressibility in comparison to the other lubricants. Figure 8(b) shows the bulk modulus for the different types of liquid lubricants at various pressure levels. The three lubricants; mineral oil with additive R300 and R800, and the pure mineral oil CR5, have approximately the same bulk modulus.

The results from testing of the lubricant compressibility at elevated pressures revealed that the lubricant bulk modulus is independent of lubricant viscosity, see Table 3 for the different lubricant viscosities. Although a direct effect of lubricant viscosity with increasing lubricant pressure build up was not taken into account in the study, it is noticed that larger viscosity

lubricants (see Table 3) do not provide larger bulk modulus. The lubricant TDN81, which has medium viscosity, has the largest bulk modulus, whereas the oils R800, R300 and CR5 have approximately the same, lower bulk modulus. The mixed oil CR5-Sun has slightly lower bulk modulus than those.

A non-linear increase in bulk modulus with pressure is observed. At lower pressures, the bulk modulus increases more rapidly than at higher pressures. The bulk modulus at 500 MPa is about 2 to 2.5 times larger than at ambient pressure, and the compression of the lubricant is about 13 to 15 percent. The present results are in good agreement with findings in literature by Lindqvist and Hoglund, (1995) using a split-hopkinson pressure bar method. In modelling of MPHSL, the compressibility of the lubricants versus pressure is an important input data if the pressure distribution and friction is to be calculated. The trapped lubricant may have escaped from the pockets if the trapped lubricant generates a larger pressure than the sealing pressure between the lubricated workpiece and the die (Bech et al., 1999) by the earlier mentioned MPHDL mechanism. Prediction of this also requires data on the lubricant bulk modulus.

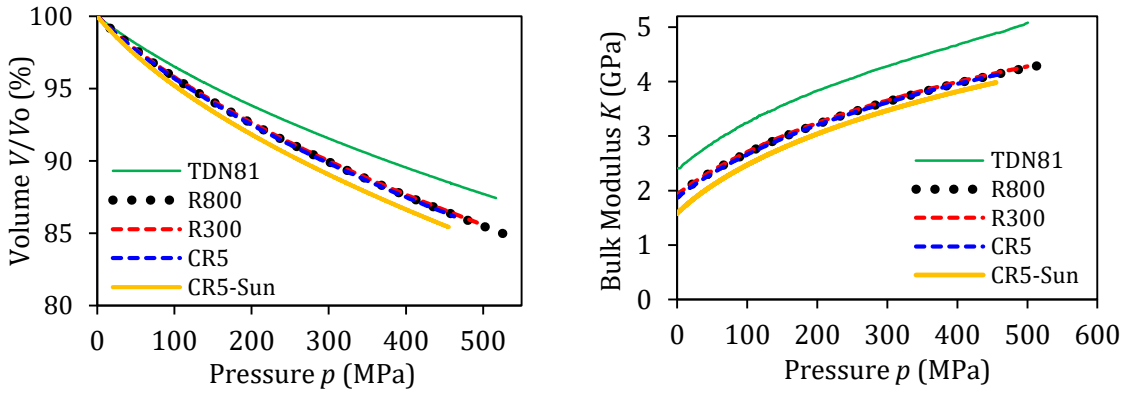

Figure 8: (a) Relative volume V/V_o, and (b) Bulk modulus K of the test lubricants at increasing pressure.

6.3 Comparison of the experimentally measured lubricants with models regarding relative density

Comparison of the lubricant compressibility results with theoretical predictions are discussed in this section. The measured datas are fitted to the Tait Equation of State (EoS) (Bair et al., 2016) and to the Dowson and Higginson model (Tuomas and Isaksson, 2006). It is observed in Figure 9 that the experimentally measured lubricants, TDN81, R800 and CR5-Sun, are best fitted to the Tait EoS in comparison to the Dowson-Higginson model. The experimental measurement fit the Tait EoS before the liquid lubricant solidifies. The fit seems to be acceptable only up to a presure of about 500 MPa. The measured liquid lubricants, TDN81 and R800, can be seen to be less compressible than the CR5-Sun and the Tait EoS for the neat oil. These findings were as expected, since the mineral oil with no additives, CR5-Sun, does not promote MPHSL lubrication and has no boundary lubrication properties, whereas the mineral oil, R800 and TDN81, may support micro-hydrodynamic lubrication and these two mineral oils furthermore has boundary lubricating

properties. The slightly better compressibility performance of the TDN81 compared to the R800 further supports the hypothesis of micro-hydrodynamic effects (Sulaiman et al., 2017).

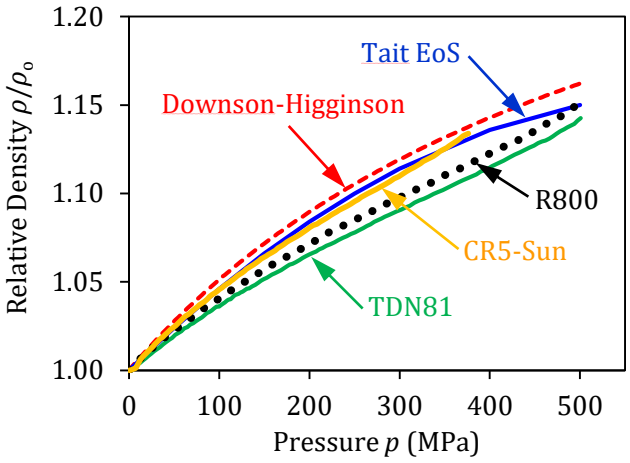

Figure 9: Relative density as a function of pressure of the measured liquid lubricants, TDN81, R800 and CR5-Sun, compared with the Tait EoS and Downson-Higginson models for the neat oil.

7.0 CONCLUSION

The experimental procedure for determining lubricant bulk modulus by a more advanced laboratory test based on a newly designed high-pressure equipment has proven to work satisfactorily up to a pressure of 500 MPa. The lubricant compressibility experiment with a direct pressure measurement inside the high-pressure container allows for the direct determination of the bulk modulus at various pressure levels with no influence from friction between punch and container in the sealing. Using water as a reference, a good agreement has been established between the experimental bulk modulus and values suggested in literature. Testing of liquid lubricants has revealed a nonlinear relationship between the bulk modulus and the pressure. The experimentally measured lubricants were best fitted to the Tait EOS model. Despite the frequent assumption that liquid lubricant is incompressible, the present study proved that the liquid lubricants have some degree of compressibility. The lubricant compressibility is especially pronounced when applying high pressure to a lubricant that is confined between two solid surfaces, where a significant amount of energy can be expended to compress the lubricant, and therefore squeezing the lubricant molecules closer together.

ACKNOWLEDGEMENT

The work is supported by the Danish Council for Independent Research (Grant no.: DFF–4005–00130). M.H. Sulaiman also would like to thank the Universiti Malaysia Perlis, the Ministry of Education, Malaysia, via Grant no. 9009-00059 and the Taiho Kogyo Tribology Research Foundation (TTRF) (Grant no.: 9008-00015).

REFERENCES

ASTM D6793. Standard Test Method for Determination of Isothermal Secant and Tangent Bulk Modulus.

Azushima, A. (2000). FEM analysis of hydrostatic pressure generated within lubricant entrapped into pocket on workpiece surface in upsetting process. Journal of Tribology, 122, 822–827.

Azushima, A., & Kudo, H. (1995). Direct observation of contact behaviour to interpret the pressure dependence of the coefficient of friction in sheet metal forming. CIRP Annals - Manufacturing Technology, 44, 209–212.

Azushima, A., Tsubouchi, T., & Kudo, H. (1990). Direct observation of lubricant behaviors under the micro-PHL at the interface between workpiece and die. Proceedings of 3rd International Conference on Technology Plasticity, 1, 551–556.

Bair, S., Baker, M., & Pallister, D.M. (2016). Revisiting the compressibility of oil/refrigerant lubricants. Journal of Tribology, 139, 1–4.

Bech, J., Bay, N., & Eriksen M. (1998). A study of mechanisms of liquid lubrication in metal forming. CIRP Annals - Manufacturing Technology, 47, 221–226.

Bech, J., Bay, N., & Eriksen, M. (1999). Entrapment and escape of liquid lubricant in metal forming. Wear, 232, 134–139.

Ceron, E., Olsson, M., & Bay, N. (2014). Lubricant film breakdown and material pick-up in sheet forming of advanced high strength steels and stainless steels when using environmental friendly lubricants. Advanced Materials Research, 967, 219–227.

Hayward, A.T.J. (1967). Compressibility equations for liquids: a comparative study. British Journal of Applied Physics, 18, 965–977.

Jacobson, B.O., 1991. Rheology and elastohydrodynamic lubrication. Elsevier: New York, 1–382.

Kudo, H. (1965). A note on the role of microscopically trapped trapped lubricant at the tool-work interface. Journal of Mechanical Sciences, 7, 383–288.

Kudo, H., Tsubouchi, M., Takada, H., & Okamura, K. (1982). An investigation into plasto-hydrodynamic lubrication with a cold sheet drawing test. CIRP Annals - Manufacturing Technology, 31, 175–180.

Lindqvist, S., & Hoglund, E., 1995. Compressibility and density of lubricants in transient loading. PhD Thesis, Lulea University of Technology.

Lo, S-.W., & Wilson, W.R.D. (1999). A theoretical model of micro-pool lubrication in metal forming. Journal of Tribology, 121, 731–738.

Mizuno, T., Okamoto, M. (1982). Effects of lubricant viscosity at pressure and sliding velocity on lubricating conditions in the compression-friction test on sheet metals. Journal of Lubrication Technology, 104, 53–59.

Nellemann, T., Bay, N., & Wanheim, T. (1977). Real area of contact and friction stress - the role of trapped lubricant. Wear, 43, 45–53.

Ohno, N. (2007). High pressure behaviour of toroidal CVT fluid for automobile. Tribology International, 40, 233–238.

Sorensen, C.G., Bech, J.I., Andreasen, J.L., Bay, N., Engel, U., & Neudecker, T. (1999). A basic study of the influence of surface topography on mechanisms of liquid lubrication in metal forming. CIRP Annals - Manufacturing Technology, 48, 203–208.

Stephany, A., Le, H.R., Sutcliffe, M.P.F. (2005). An efficient finite element model of surface pit reduction on stainless steel in metal forming processes. Journal of Materials Processing Technology, 170, 310–316.

Sulaiman, M.H., Christiansen, & Bay, N. (2017). A study of DLC coatings in ironing of stainless steel. Proceedings of 36th International Deep Drawing Research Group (IDDRG) conference.

Sulaiman, M.H., Christiansen, P., Martins, P.A.F., & Bay, N. (2016). Determination of lubricant bulk modulus in metal forming by means of a simple laboratory test and inverse FEM analysis. Proceedings of 7th International Conference on Tribology in Manufacturing Processes, 316–323.

Sulaiman, M.H., Christiansen, P., Bay, N. (2017) The influence of tool texture on friction and lubrication in strip reduction testing. Lubricants, 5, 1–11.

Sulaiman, M.H., M.H., Christiansen, P., Bay, N. (2017) The influence of tool texture on friction and lubrication in strip reduction. Proceedings of 12th International Conference on Technology of Plasticity (ICTP), 2263–2268.

Sulaiman, M.H., Christiansen, & Bay, N. (2018). A study of anti-seizure tool coatings in ironing of stainless steel. Jurnal Tribologi, 17, 1-14.

Sundström, B., 1998. Handbok och formelsamling i Hållfasthetslära (in swedish), KTH.

Tuomas, R., Isaksson, O. (2006). Compressibility of oil/refrigerant lubricants in elasto-hydrodynamic contacts. Transaction of ASME, 128, 218–220.

Wanheim, T., (1973). Friction at high normal pressures. Wear, 25, 225–244.